Iran Polym J (2017) 26:711–720
DOI 10.1007/s13726-017-0556-7

ORIGINAL PAPER

Clay-hyperbranched epoxy/polyphenylsulfone nanocomposite membranes

Mehdi Mahmoudian[1] · Peyman Gozali Balkanloo[1]

Received: 14 November 2016 / Accepted: 2 August 2017 / Published online: 12 August 2017

Abstract Nanocomposite membranes containing polyphenylsulfone (PPSU) and a clay modified with a hyperbranched epoxy (HBE) were prepared by blending of modified montmorillonite (m-MMT) with a polymer solution using phase inversion method. The hyperbranched epoxy synthesized by polycondensation reaction of bisphenol A and triethanolamine with epichlorohydrin was grafted to amine-functionalized MMT by reaction between the epoxy groups of hyperbranched epoxy and the amine groups on the MMT surface. In this way, the m-MMT was exfoliated into single layers of nanoparticles in a solvent medium and the polymer chains were intercalated into m-MMT layers. The aim was to study the effect of this additive on the membrane separation efficiency. For this purpose, pure water flux, fouling, and pigment and heavy metal rejection were measured by a home-made dead end filtration cell and the performance of the prepared membranes was investigated. Hydrophilicity of the nanocomposite membranes was specified by water contact angle measurements. Degree of dispersion of additive into the polymer matrix and membrane morphology were studied by FESEM. Membrane surface area, pore size, and volume were evaluated by BET. The results indicated that the surface hydrophilicity increased after incorporation of m-MMT. Furthermore, the water permeability, salt rejection, and antifouling resistance of PPSU membranes were improved significantly. Membrane with 3 wt% m-MMT showed the best performance compared to other membranes.

✉ Mehdi Mahmoudian
m.mahmoudian@urmia.ac.ir

[1] Nanotechnology Research Institute, Urmia University, P.O. Box: 57159-404931 Urmia, Iran

Keyword Montmorillonite · Polyphenylsulfone · Nanocomposite membranes · Hyperbranched epoxy

Introduction

In recent years, due to the release of a variety of contaminants into the environment, great efforts have been made in removing them. Pollution of water resources by man has caused great concern over various toxic compounds such as organic compounds, dyes, heavy metals, and pesticides released in water. These compounds usually are water soluble and the separation processes associated with them have always been faced with complexity [1]. One of the common ways to assist environmental protection, improve human health and medical concerns, especially in water purification, is based on membrane technology which is very effective and low cost [2–4].

Polysulfone (PSf)-based membranes are used most extensively in membrane processes because of their high heat resistance, chemical, and mechanical strength and stability over a wide range of pH [5]. Generally, the membranes with antifouling performance have short service life. Low surface hydrophilicity and adsorption of soluble hydrophobic materials create fouling phenomenon and lower the permeability in membranes. The major drawback of polysulfone-based membranes is that they are hydrophobic in nature as well, which makes them susceptible to fouling [6, 7].

In the last few decades, nanocomposite membranes based on fillers such as carbon nanomaterials and inorganic clays have been highly regarded due to their unique characteristics. Compared to neat membranes, these novel nanomaterials, applied in the field of membranes, can largely improve properties such as the operating temperature and pressure, chemical stability, selectivity, permeability, and also can

reduce the fouling tendency [8, 9]. One of the most widely employed methods for increasing the surface hydrophilicity is blending the polymer with modifiers such as inorganic clays [10, 11], graphene oxide [12, 13], carbon nanotubes [14, 15], or a mix of them [16]. Anadão et al. showed that the hydrophilicity of PSf membrane increases by blending of PSf with unmodified montmorillonite and it was an evidence for improved performance achieved due to increasing the hydrophilicity [17]. Vatanpour et al. and Daraei et al. improved hydrophilicity and antifouling property of polyethersulfone composite membranes using functionalized multi-walled carbon nanotubes (MWCNT) as modifiers [18, 19]. Kumar et al. modified polysulfone with polymer-grafted bentonite for ultrafiltration of oily waste water and obtained up to 98% oil rejection [20]. Ghasemi et al. [21] utilized graphene oxide as an additive to obtain a nanocomposite membrane for water treatment. The membrane with 3 wt% additive showed the best result for rejection of impurities. Arockiasamy Dass et al. [22] fabricated polyphenylsulfone-based mixed matrix hollow fiber membranes to investigate separation of proteins and antifouling properties. Their experimental results showed that the addition of hydrophilic nanoparticles to polyphenylsulfone improved the thermal and mechanical properties, permeability, and altered the surface and sub-structure properties of the produced hollow fiber membranes.

Clay mineral is a multilayer compound composed of two silica tetrahedral plates with an alumina octahedral central structure. In the silicate layers, silicon atoms are linked together by oxygen linkages and cations such as sodium, magnesium, calcium ions, or water molecules which filled the gaps between the sheets [23]. Ceramic materials have been used as fillers in membranes, and their nanometric properties have been explored for producing nanocomposite membranes with enhanced performance [24, 25].

Modification of these materials is essential for improving their performance in membranes [26]. Incorporation of modified montmorillonite into the membrane's structure was caused to make a porous and more hydrophilic filter, which could be used in ultrafiltration membranes [27]. The main advantages of the nanocomposite membranes made by incorporation of these nanofillers are high surface area, low cost and, more importantly, their considerably improved physicomechanical properties [28].

Modification of montmorillonite enhanced the distances between the layers and led to high interactions between the polymer matrix and the dispersed modified clay layers [29, 30]. A modified montmorillonite with the surface negative charges stable throughout an entire pH range can show very interesting properties in membranes.

Keeping this in view, in the present work, a montmorillonite modified with a hyperbranched epoxy (HBE) was used to improve the polyphenylsulfone (PPSU) membrane's performance. To the best of our knowledge, HBE–MMT has not been used, to date, for fabricating nanocomposite membranes. The synthesized HBE–MMT nanomaterial was blended with the PPSU matrix membrane by phase inversion method.

Experimental

Materials

Polyphenylsulfone (M_w 50,000 and 1.28 specific gravity) was supplied by BASF. *N*-Methyl-2-pyrrolidone (NMP), montmorillonite, (3-aminopropyl)triethoxysilane (APTES), epichlorohydrin, triethanolamine, bisphenol A, sodium hydroxide and bovine serum albumin (BSA, M_w 67.000) were provided from Sigma-Aldrich. Dimethyl sulfoxide (DMSO) was obtained from Merck. All other reagents used in the present investigation were reagent grades.

Preparation of hyperbranched epoxy

Bisphenol A (2.5 g), triethanolamine (0.25 g), and epichlorohydrin (4.99 g) were added in a two-neck round-bottom flask. The reaction mixture was stirred with a magnetic stirrer at 110 °C and a 5 N aqueous solution of NaOH (1.08 g) (equivalent to the hydroxyl group) was added slowly by a dropping funnel for 60 min. After 4 h, the reaction mixture was cooled to ambient temperature, transferred to a separating funnel and allowed the aqueous layer to separate from the desired organic layer. The collected organic layer was washed with 15% aqueous sodium chloride solution and distilled water 2–3 times, respectively. Finally, the viscous sticky transparent product was filtered and dried at 80 °C under vacuum for 24 h.

Modification of montmorillonite

To achieve better modification performance, at first the distance between the layers of montmorillonite was expanded. For this purpose, 0.33 g of montmorillonite was added into the mixture of 6 mL of DMSO and 1 mL of water under reflux and stirred vigorously for 24 h. The product was maintained at room temperature for 12 h. The obtained material was centrifuged and washed three times with ethanol to remove excess DMSO. The product was dried in an oven at 60 °C for 24 h.

An amount of 2 g of the obtained product was added to 10 mL of APTES and under N_2 atmosphere it was refluxed at 200 °C and vigorously stirred for 48 h. The obtained product was separated and washed six times with toluene and dried at 80 °C for 12 h.

0.5 g of MMT–APTES was added into a mixture of 50 mL of THF and 25 mL of water in a two-neck flask and dispersed with an ultrasonic device. At this stage, 6.0 g of hyperbranched epoxy was dissolved in 50 mL of THF and added into the mixture. Next, the system was exposed to nitrogen flow for 1 h at 80 °C and maintained in reflux condition for 48 h. Finally, the sample was centrifuged and the obtained solid was washed several times with THF to a neutral pH and then placed in a vacuum oven to be dried for 24 h at 60 °C.

Nanocomposite membrane preparation

The membranes were prepared by classical phase inversion method using PPSU and PEG as solute material, NMP as solvent, functionalized montmorillonite (HBE–MMT) as additive, and distilled water as non-solvent (coagulation bath). Certain amounts of polysulfone (2 g) and polyethylene glycol (PEG, M_w 3000) (1 g) were dissolved in NMP (~7 g), at 60 °C for 24 h and stirred to obtain a homogenous solution. Different percentages of dispersed HBE–MMT (0, 1, 3, 5, 7 wt% based on the weight of PPSU) were added into the solution (1 g) and dispersed by a UP100H-Hielscher ultrasonic homogenizer (Table 1). The casting solution was flattened on clean and dry glass plates with 200 µm thickness and maintained at room temperature for 30 s before being immersed into a coagulation bath (distilled water) for 5 min. After peeling off from the glass plates, the resultant membranes were rinsed in distilled water and then stored in slightly chlorinated distilled water and used for further characterization and filtration tests.

Characterization

Proton nuclear magnetic resonance (Bruker Advance DPX-250 MHz spectrometer) (^{1}H-NMR) and Fourier transform infrared spectroscopy (Bruker IFS-66/S FTIR) (FTIR) were used to confirm the HBE synthesis. Hitachi (S4160) field emission scanning electron microscopes (FESEM) were used to inspect the cross section and surface morphology of the prepared membranes. The membranes were cut into small pieces. The pieces were immersed in liquid nitrogen for 10–15 s for freezing. Later, the membranes were broken and dried. The dried samples were sputtered by a gold layer to be electrically conductive. The UV–visible spectra of different solutions were monitored on a UV–Vis spectrophotometer (CARRY100 Bio 5). BET and BJH tests were used to evaluate the surface area, pore size, and volume of the membranes by a Belsorp Mini instrument. Heavy metal removal was determined by a Shimadzu AA-670 atomic absorption spectrophotometer with a hallow cathode lamp using an air–acetylene flame. For determination of the water contact angle, deionized water was dropped onto the membrane surface with a microsyringe, and the contact angle was measured after stabilizing the water drop (OCA 15 plus, Dataphysics, Germany).

Table 1 Casting solution compositions used in preparation of PPSU/HBE–MMT membranes

Entry	Casting solution			
	HBE–MMT (wt%)	PPSU (g)	PEG (g)	NMP (g)
1	0	2	1	7
2	1	2	1	6.98
3	3	2	1	6.94
4	5	2	1	6.90
5	7	2	1	6.86

Membrane performance evaluation

Pure water flux (PWF)

The pure water flux of all membranes was measured using a self-fabricated lab-scale filtration unit. The membranes were maintained in water for 24 h before carrying out the experiments. The circular membrane sample with 3.6 cm^2 area was placed inside the sample holder. Next, the pure water flux was measured at 5, 7 and 9 bar, respectively, by collecting the filtrated water. For each membrane, average value was reported from three trials. The pure water flux was calculated using the equation:

$$J_W = \frac{Q}{A.\Delta T}$$

where pure water flux (J_w) is expressed in L/m^2h and Q is the quantity of water collected over a period of 5 min (Δt) and A(m^2) is the surface area unit.

Rejection of salt, heavy metal, and dye

Rejection percentage of salt, heavy metal or dye was calculated using the following equation:

$$R\% = \left(1 - \frac{C_p}{C_f}\right) \times 100$$

where C_p and C_f are the concentrations (salt, heavy metal or dye) in the permeate and feed, respectively. The concentrations of salt in the feed and permeate were evaluated by conductometry. Three salts including NaCl, $MgSO_4$, and Na_2SO_4 were evaluated (salt concentration in the feed was 0.01 molar at 5 bar pressure). Dye rejection tests were performed by methylene blue (MB) and methyl orange (MO) solutions with an initial concentration of 0.0005 molar. The

concentration of dye in the permeate was determined by UV spectrophotometry. The heavy metal rejection was determined using an aqueous solution of $ZnSO_4{\cdot}7H_2O$ (10 ppm), Ni $(NO_3)_2{\cdot}6H_2O$ (100 ppm), $CuSO_4{\cdot}5H_2O$ (1000 ppm), and Cd $(NO_3)_2{\cdot}4H_2O$ (2500 ppm). The pressure was 5 bar and the testing time was 60 s for each membrane.

Antifouling properties

The antifouling property of the membranes was determined using a bovine serum albumin (BSA) solution in PBS buffer (100 ppm, 50 mM, pH 7). Each membrane was compacted for an initial 20-min period at 5 bar until reaching an equilibrium condition in water, while the pure water flux was maintained in a constant value. The pressure was reduced to 4 bar and the pure water flux of the membrane, J_{w1} (kg/m^{2}h), was determined over a period of 1 min. After completion of the pure water flux measurement, BSA was fed inside the permeation cell to be filtered through the membrane for 30 min. Then, the membrane was flushed with pure water for 15 min and pure water flux, J_{w2} (kg/m^{2}h), was measured again. For each membrane, J_{w1} and J_{w2} were measured twice. Finally, the membrane antifouling property was determined by calculating flux recovery ratio (FRR) using the following equation:

$$\mathrm{FRR}(\%) = \frac{J_{W2}}{J_{W1}} \times 100$$

The concentrations of BSA in the feed and permeate were measured using a UV spectrophotometer at a wavelength of 280 nm. The samples were treated with Bradford reagent and kept for 10 min prior to measuring their concentrations. The percent of BSA rejection was calculated using the following equation:

$$\%\mathrm{SR} = \left(1 - \frac{C_p}{C_f}\right) \times 100$$

where C_p (mg/mL) and C_f (mg/mL) designate the concentrations of BSA in the permeate and feed, respectively.

Finally, to examine biofouling resistance of the membranes, the modified and neat membrane samples were subjected to the static protein absorption test. For this purpose, samples were cut in square shape with 0.5 cm^2 specific surface area and then ultrasonically treated (100 W, 40 kHz) in a phosphate buffer solution (PBS, pH 7.0, 0.1 M) for 5 min, and then incubated in a BSA–phosphate buffer solution (1.0 mg/mL) at 25 °C for 24 h. Afterwards, the samples were rinsed three times using PBS, and then treated in PBS under ultrasonic condition for 2 min to remove the adsorbed protein from the surface. The amounts of protein absorbed on the membranes were determined by UV spectroscopy.

Results and discussion

Characterization of HBE and HBE–MMT

The hyperbranched epoxy was synthesized by polycondensation reaction of bisphenol A and triethanolamine with epichlorohydrin and it was grafted to the amine-functionalized MMT via the reaction between the epoxy groups of hyperbranched epoxy and amine groups present on the surface of MM. Fourier transform infrared (FTIR) test was used to characterize the modified MMT functional groups. The FTIR spectra of MMT, APTES–MMT, and HBE–MMT can be seen in Fig. 1. The characteristic bands of MMT (1) were observed at 527, 798, and 1054 cm^{-1} which were attributed to the Al–O–Al, Al–OH–Mg, and Al–OH–O–Si vibrations, respectively. For APTES–MMT (2), in addition to the bands of MMT, new characteristic bands appeared at 1489, 1563 cm^{-1} (N–H vibrations), and 2939 cm^{-1} (bending vibration of aliphatic C–H). The functionalization of MMT with HBE was confirmed by FTIR (3). The decreasing peak intensity at 3622 cm^{-1} (N–H vibrations) was related to the amine groups reacted with HBE. The appearance of the peaks at 3102.19 and 1250.63 cm^{-1} was attributed to the =C–H in aromatic ring and in epoxy ring, respectively.

The structure of the hyperbranched epoxy resin was confirmed by ^{1}H-NMR (400 MHz, $CDCl_3$, Me_4Si), and revealed the characteristic peaks at 3.74–3.82 (2H, m, NCH_2CH_2OH), 2.57 (2H, t, NCH_2), 1.65 (3H, s, CH_3), 6.82 (4H, d, Ph), 7.14

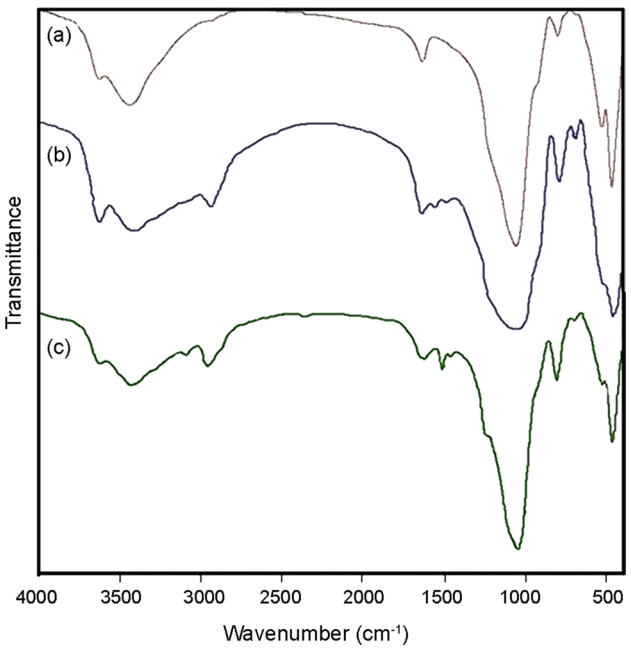

Fig. 1 FTIR spectrum of **a** MMT, **b** APTES–MMT, and **c** HBE–MMT

(4H, d, Ph), 4.12 and 4.18 (2H, d, OCH_2), and 4.40 (1H, m, CHOH), according to the literature (Fig. 2) [31].

Characterization and performance of membrane

The membranes were prepared by phase inversion method using PPSU as polymer, PEG as pore-forming agent, and modified MMT (1, 3, 5, and 7 wt%) as additive. Due to the presence of functional groups on the surface of modified MMT, it could efficiently be incorporated into the polymer casting solution and enhanced the surface hydrophilicity of the membrane. However, the flat MMT sheets might be helpful to reject the solute molecules effectively. To evaluate the membrane performance, the effect of additive amounts with respect to morphology, hydrophilicity, flux, antifouling, salt rejection, and dye rejection was investigated.

Membrane morphology

Both cross-sectional and surface morphology of membranes were examined in detail by FESEM. The FESEM micrographs of the cross sections for the neat and modified PPSU membranes are shown in Fig. 3. Additive concentration as an effective factor influenced the nanocomposite membrane morphologies. The finger-like structures were influenced by the percentage of additive added. More finger-like macrovoids were observed in the membranes with higher amount of modified MMT which could be attributed to the rapid exchange of solvent with non-solvent during the phase inversion process due to the presence of highly hydrophilic groups on the modified MMT [32]. By increasing the additive concentration in the modified MMT as a solid and hydrophilic material, there developed thermodynamic instability in casting solution and consequently the flow rate of water increased and led to the expansion of macrovoids. However, the clay acted as a surfactant and reduced the interfacial tension between water and membrane dope which affected the exchange rate of solvent and non-solvent and precipitation kinetics during phase inversion. This in turn, changed the membrane morphology [33]. The surface micrographs of neat and modified PPSU membranes indicated that the clays were dispersed in the PPSU matrix in the form of large and small aggregates. It was difficult to estimate the size of the aggregates because they were non-isometric and randomly dispersed in the matrix. The clay particles were dispersed in the form of small aggregates or even as individual particles (Fig. 4). Additionally, as can be seen clearly in the FESEM images, the increase of MMT–HBE has resulted in a rise in the amount of the particles on the membrane surface.

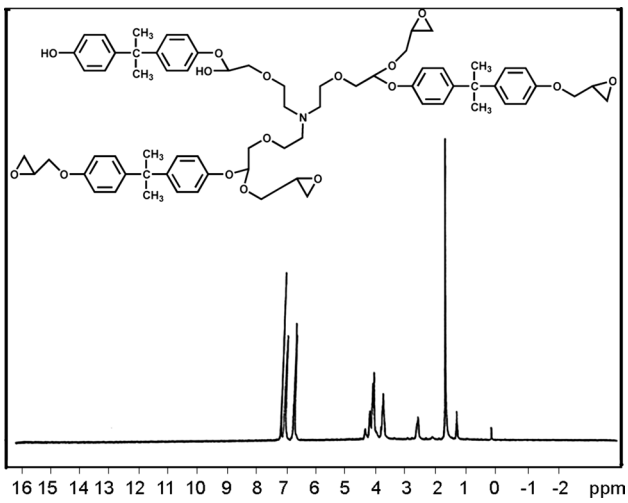

Fig. 2 ^{1}H-NMR spectrum of the hyperbranched epoxy

BET surface area, BJH pore size, and volume analyses

The results of the BET and BJH analyses for the membranes with 1–7 wt% of HBE–MMT are given in Table 2. By increasing the additive amount, the surface area and pore volume enhanced intensively to 3% (as shown in FESEM micorographs) and then decreased slightly, but the pore size radius remained almost unchanged. At high percentage of additive, a decrease in the specific surface area and pore volume may be due to the effect of the filling material in the polymer matrix. To investigate the pressure effect, the membrane with 3% HBE–MMT was pressed under 10 bar pressure for 30 min and the BET analysis was repeated. As seen in the table, the surface area and pore volume only decreased slightly, representing the compressive strength of the membrane.

Pure water flux of membranes

It is possible to verify that the use of additives affects membrane permeability. As it was expected, the permeate fluxes increased easily by increasing the transmembrane pressure for all the membranes. The water flux of the modified membranes was remarkably higher than that of the neat PPSU membrane. The surface hydrophilicity of the modified membranes enhanced and a large number of finger-like macrovoids were obtained. The improvement in the pure water flux of nanocomposite membranes was attributed to (1) the high water-holding capacity of the membranes and the ease of transport of water through the membranes, and (2) the interfacial gaps between the layered additive and the polymer matrix for additional water channels [34]. On the other hand, by increasing the modified clay content by over 3%, the particles aggregated, and the effective surface area decreased (Fig. 5).

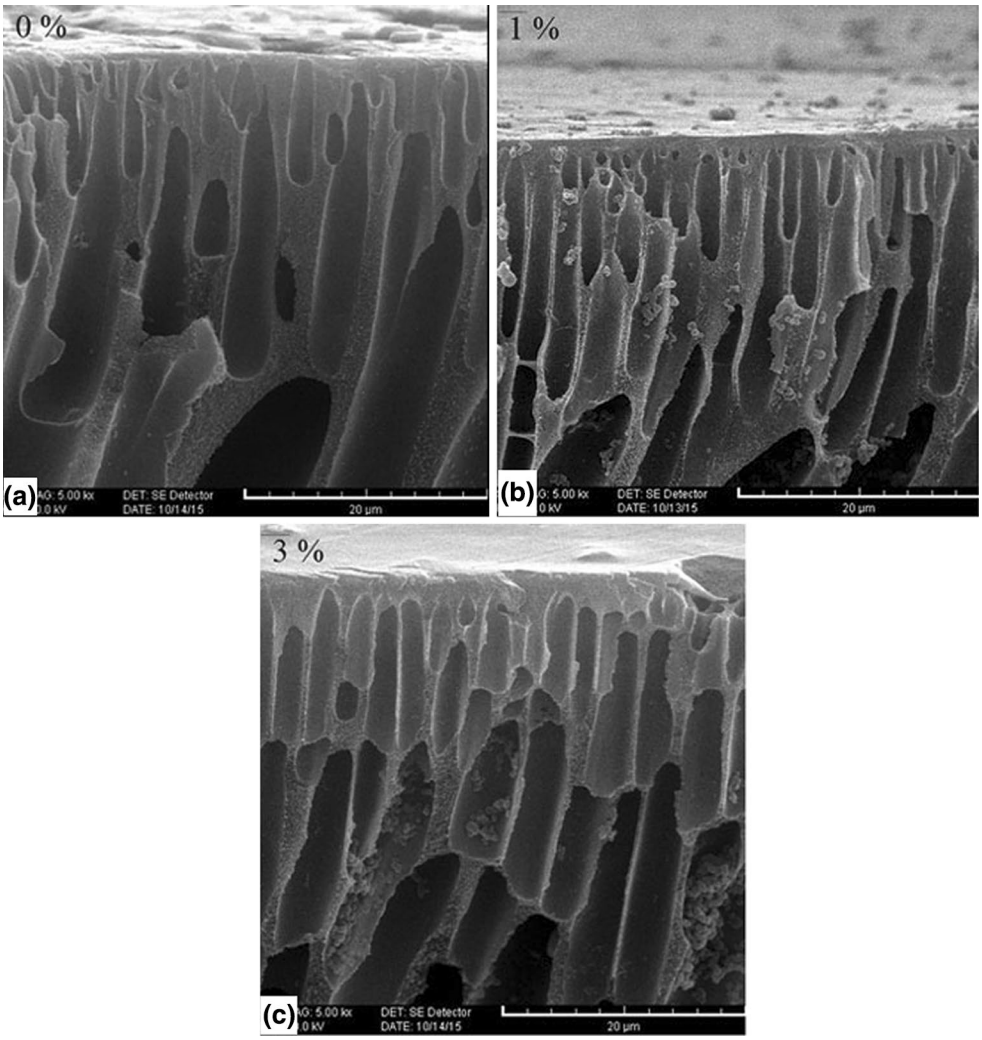

Fig. 3 Cross-sectional FESEM images of the modified MMT/PPSU membranes (modified MMT—**a** 0%, **b** 1%, and **c** 3%)

Salt rejection

The salt rejection performances of the prepared nanocomposite membranes are shown in Fig. 6. The rejection performances of all of the modified membranes were more than that of the neat PPSU membrane. The salt rejection was in the order of NaCl < Na_2SO_4 < $MgSO_4$. The effective factors affecting the salt rejection of membrane are size exclusion (steric effects) [35], Donnan exclusion (electrical repulsion) [36], concentration polarization [37], and mobility which is determined by diffusion coefficient and effective size of ions [38]. Therefore, the higher rejection obtained with $MgSO_4$ in comparison with NaCl and Na_2SO_4 was ascribed to the steric effects [39, 40]. The increase in modified clay additive concentration from 1 to 3 wt% improved the salt rejection and also water permeability due to increased porosity of the membrane [41]. Other reports also showed that both water flux and rejection were improved by embedding additives [42].

Dye removal

The modified PPSU membranes were used for removing methyl orange (MO) and methylene blue (MB) from wastewater because of a suitable membrane pore size, dye size, high ionic charge density in the surface, and lack of requirement for pH tuning. The nanocomposite membranes significantly exhibited a higher dye removal capacity than pure PPSU. By increasing the modified clay content up to 3%, the dye removal percent increased in both dyes. The additive particles aggregated and the porosity and effective surface area decreased with the increase in additive content by over 3%. Therefore, the dye removal percent decreased for the membranes with

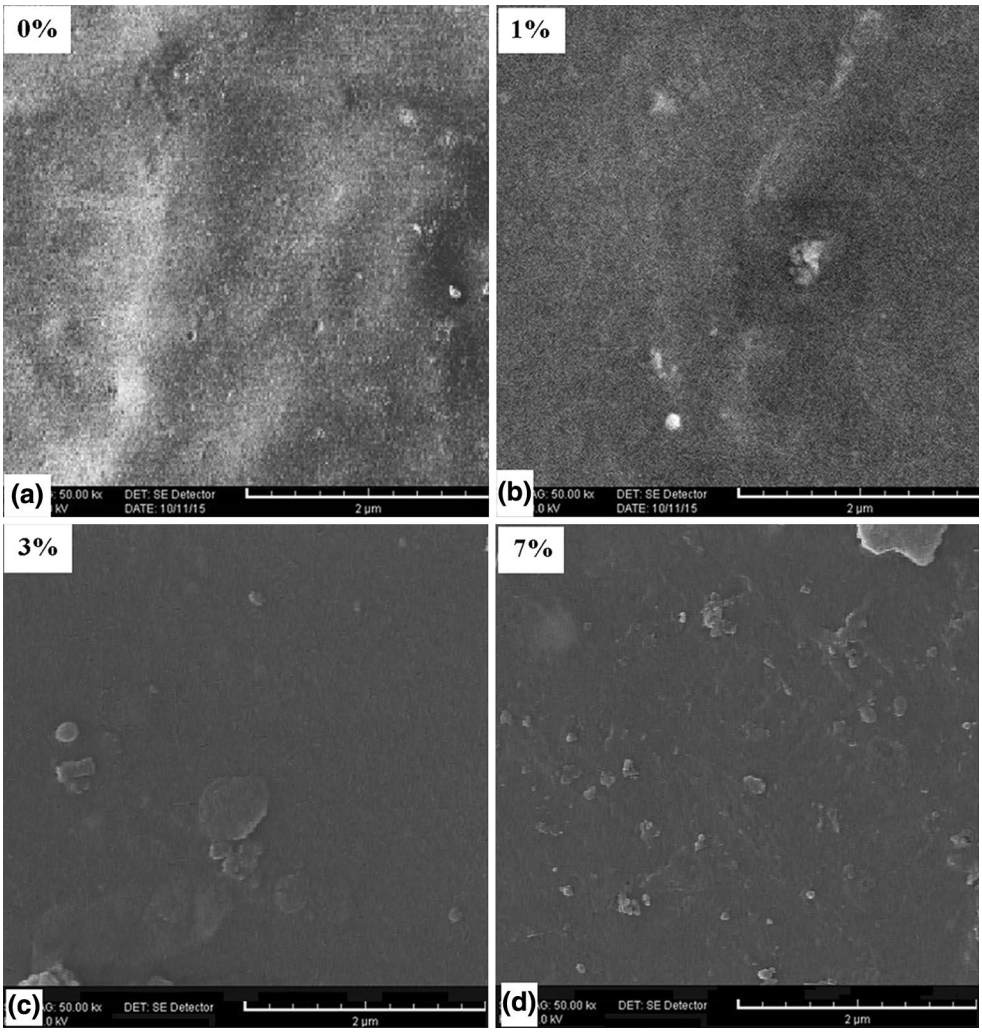

Fig. 4 FESEM surface images of **a** neat; **b**, **c**, and **d** the modified-MMT/PPSU membrane

Table 2 BET and BJH analyses of modified MMT/PPSU membrane

Additive parameter (%)	1%	3%	5%	7%	3% (under pressure)
Efficient surface area (m^2/g)	4.11	24.95	21.2	17.2	23.30
Pore volume (cm^3/g)	0.016	0.100	0.034	0.030	0.096
Pore size—radius (nm)	1.22	1.22	1.63	1.60	1.22

more than 3% additive. Importantly, the higher percent removal of MO compared to MB could be attributed to its negative charge; a membrane negative charge due to HBE with negative charge led to Donnan exclusion effect (electrical repulsion (Fig. 7).

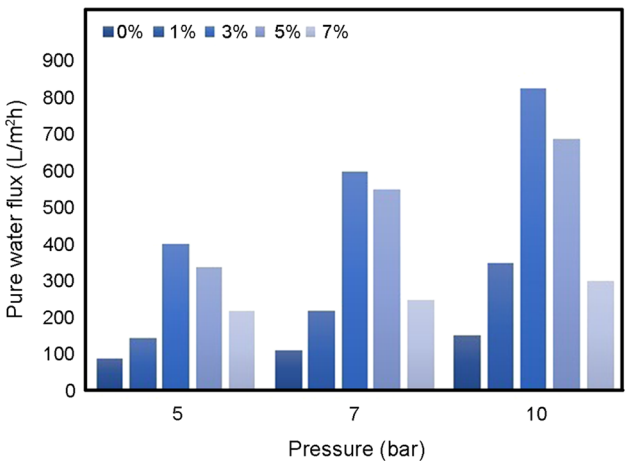

Fig. 5 Pure water flux of neat PPSU and modified membranes

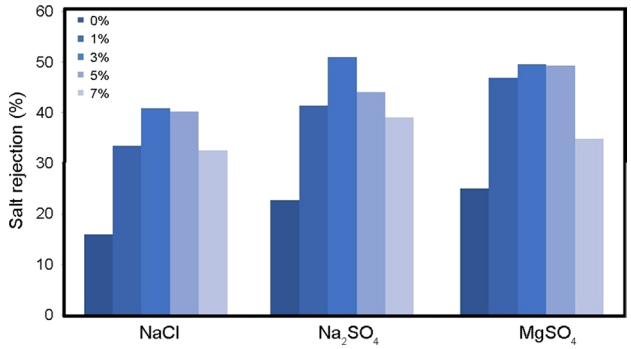

Fig. 6 Salt rejection performance of the prepared nanofiltration membranes

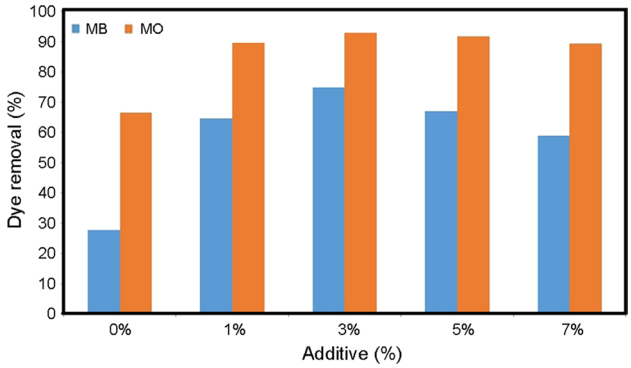

Fig. 7 Dye removal of membranes containing modified MMT

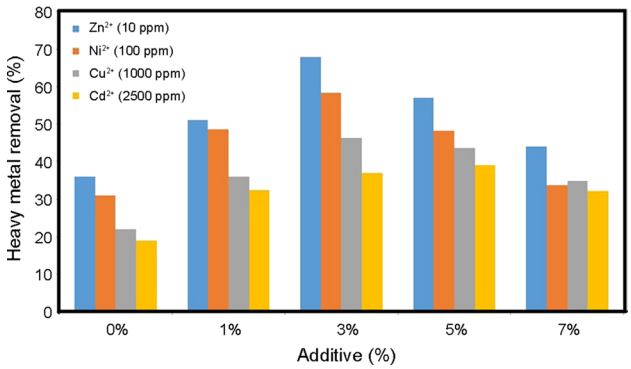

Fig. 8 Heavy metal removal of HBE–MMT/PPSU membrane

Heavy metal removal

The heavy metal removal performances of the prepared nanocomposite membranes exposed to $ZnSO_4.7H_2O$, $Ni(NO_3)_2.6H_2O$, $CuSO_4.5H_2O$, and $Cd(NO_3)_2.4H_2O$ solutions are shown in Fig. 8. The removal workings of all the modified membranes were higher than that of the neat PPSU membrane. The nanocomposite membrane with 3 wt% additive showed the best performance. The heavy metal removal was in the order of Zn > Ni > Cu > Cd, which could be attributed to size exclusion (steric effects) and mobility, which are usually affected by the diffusion coefficient and effective ionic size.

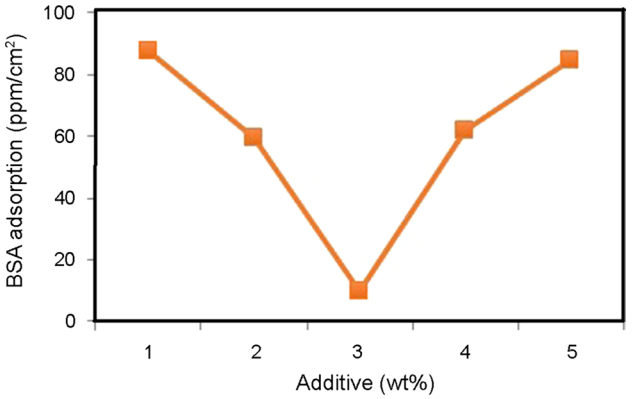

Fig. 9 BSA adsorption membranes in different concentrations of additive

Hydrophilic/hydrophobic nature of membranes

Contact angle reflects the hydrophilic/hydrophobic nature of the surface of a membrane and strongly influences the adsorption and transmission of permeate molecules. Compared with the neat PPSU membranes, the hybrid membranes displayed lower contact angles due to the presence of hydrophilic functional groups in HBE–MMT. The contact angle values reduced significantly from 74.3° to 53.6° when the HBE–MMT/PPSU additive percent increased from 0 to 7.0 wt% (74.3, 64.6, 62.3, 57.1, and 53.6°, respectively). This may be due to the migration of hydrophilic clay nanoplates on the membrane surface when the number of nanoplates is high.

To study the fouling properties of the membranes and effect of their additive content on fouling, the dynamic fouling analysis (flux recovery ratio) and static fouling (BSA adsorption) were performed for the fabricated membranes. Static fouling experiments were carried out using 1000 ppm solution of BSA protein in an operational pH of 7.4 at a 24-h contact time. The results of static BSA adsorption on the membrane surface are shown in Fig. 9.

According to the results, the neat PES membrane showed higher amount of BSA adsorption than the mixed nanocomposite membranes. On the other side, the increase of the modified MMT percent from 1 to 3 wt% led to lower BSA adsorption, because higher concentration of the additive increased the hydrophilicity of the membrane. The presence of tight hydration layer on the hybrid membranes is responsible for an effective reduction in the adsorbed amounts of

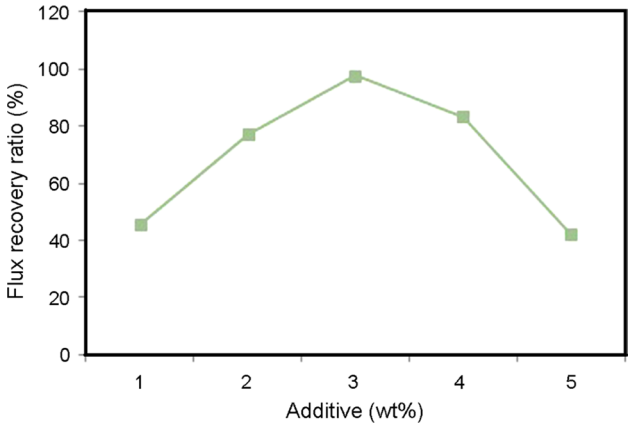

Fig. 10 Water flux recovery ratio (FRR) in different concentrations of additive

BSA, but further increasing creates rougher surface and leads to higher BSA adsorption. The results of FRR % or dynamic fouling for the membrane prepared, with and without HBE–MMT, are shown in Fig. 10. The higher flux recovery for modified membranes suggested that the protein fouling on the membrane layer was more reversible due to higher hydrophilicity of the modified membrane. The highest biofouling resistance evaluated by FRR was observed in a membrane with 3 wt% of additive. This could be related to factors such as surface hydrophilicity and roughness. The greater additive percent improved the surface hydrophilicity and meanwhile generated higher surface roughness in nanocomposite membranes.

Conclusion

HBE-clay/PPSU nanocomposite membranes were prepared through classical phase inversion method by dispersing HBE–MMT nanosheets in PPSU casting solution. The FESEM analyses showed that the addition of HBE–MMT nanosheets changed the microstructure of the PPSU membranes. The membranes exhibited greater hydrophilicity, water flux, and antifouling properties. The addition of HBE–MMT also improved the rejection of salt, heavy metals, and dyes more efficiently. It could be observed that the membrane with 3 wt% of additive had an optimal performance, while the membranes with the additive content above 3 wt% showed lower working performance.

References

1. Mbareck C, Nguyen QT, Alaoui OT, Barillier D (2009) Elaboration, characterization and application of polysulfone and polyacrylic acid blends as ultrafiltration membranes for removal of some heavy metals from water. J Hazard Mater 171:93–101
2. Peter-Varbanets M, Zurbrügg C, Swartz C, Pronk W (2009) Decentralized systems for potable water and the potential of membrane technology. Water Res 43:245–265
3. Sikdar SK, Grosse D, Rogut I (1998) Membrane technologies for remediating contaminated soils: a critical review. J Membr Sci 151:75–85
4. Sato Y, Kang M, Kamei T, Magara Y (2002) Performance of nanofiltration for arsenic removal. Water Res 36:3371–3377
5. Farrokhnia M, RashidzadehM Safekordi A, Khanbabaei G (2015) Fabrication and evaluation of nanocomposite membranes of polyethersulfone/α-alumina for hydrogen separation. Iran Polym J 24:171–183
6. Jahanshahi M, Rahimpour A, Mortazavian N (2016) Effect of polydopamine deposition conditions on polysulfone ultrafiltration membrane properties and threshold flux during oil/water emulsion filtration. Polymer 97:247–257
7. KumarS Guria C, Mandal A (2015) Synthesis, characterization and performance studies of polysulfone/bentonite nanoparticles mixed-matrix ultra-filtration membranes using oil field produced water. Sep Purif Technol 150:145–158
8. Dorraji MSS, Vatanpour V (2016) Organic-inorganic composite membrane preparation and characterization for biorefining. Membr Technol Biorefining 85–102
9. Madaeni SS, Ghaemi N, Rajabi H (2015) Advances in polymeric membranes for water treatment. Adv MembrTechnol Water Treatment 3–41
10. Felbec T, Bonk A, Kaup G, Mundinger S, Grethe T, Rabe M, Vogt U, Kynast U (2016) Porous nanoclay polysulfone composites: a backbone with high pore accessibility for functional modifications. Micropor Mesopor Mat 234:107–112
11. Yavas BH, Tanrıver N, Benli B, Kizilcan N (2015) In situ polymerization of sepiolite modified polysulfone. Procedia Behav Sci 195:2206–2209
12. Jose AJ, Alagar M (2015) Preparation and characterization of polysulfone-based nanocomposites. Manu Nanocompos Eng Plast 31–59
13. Ionita M, Pandele AM, Crica L, Pilan L (2014) Improving the thermal and mechanical properties of polysulfone by incorporation of graphene oxide. Compos Part B Eng 59:133–139
14. Khalid A, Al-JuhaniA Al-Hamouz OC, Laoui T, Khan Z, Atieh MA (2015) Preparation and properties of nanocomposite polysulfone/multi-walled carbon nanotubes membranes for desalination. Desalination 367:134–144
15. Yin J, Zhu G, Deng B (2013) Multi-walled carbon nanotubes (MWNTs)/polysulfone (PSU) mixed matrix hollow fiber membranes for enhanced water treatment. J Membr Sci 437:237–248
16. Sarfraz M, Ba-Shammakh M (2016) Synergistic effect of adding graphene oxide and ZIF-301 to polysulfone to develop high performance mixed matrix membranes for selective carbon dioxide separation from post combustion flue gas. J Membr Sci 514:35–43
17. Anadão P, Sato LF, Wiebeck H, Valenzuela-Díaz FR (2009) Montmorillonite as a component of polysulfone nanocomposite membranes. Appl Clay Sci 48:127–132
18. Vatanpour V, Madaeni SS, Moradian R, Zinadini S, Astinchap B (2011) Fabrication and characterization of novel antifouling nanofiltration membrane prepared from oxidized multiwalled carbon nanotube/polyethersulfone nanocomposite. J Membr Sci 375:284–294
19. Daraei P, Madaeni SS, Ghaemi N, Khadivi MA, Astinchap B, Moradian R (2013) Enhancing antifouling capability of PES membrane via mixing with various types of polymer modified multiwalled carbon nanotube. J Membr Sci 444:184–191
20. Kumar S, Mandal A, Guria C (2016) Synthesis, characterization and performance studies of polysulfone and polysulfone/

polymer-grafted bentonite based ultrafiltration membranes for the efficient separation of oil field oily wastewater. Process Saf Environ 102:214–228
21. GhasemiKochameshki M, Marjani A, Mahmoudian M, Farhadi K (2017) Grafting of diallyldimethylammonium chloride on graphene oxide by RAFT polymerization for modification of nanocomposite polysulfone membranes using in water treatment. ChemEng J 309:206–229
22. ArockiasamyDass L, Alhoshan M, Alam J, Muthumareeswaran Figoli A, Kumar A (2017) Separation of proteins and antifouling properties of polyphenylsulfone based mixed matrix hollow fiber membranes. Sep Purif Technol 174:529–543
23. Brigatti MF, Galan E, Theng BKG (2006) Handbook of clay science: structures and mineralogy of clay minerals. Elsevier, Amsterdam
24. Corcione CE, Cataldi A, Frigione M (2013) Measurements of size distribution nanoparticles in ultraviolet-curable methacrylate-based boehmite nanocomposites. J Appl Polym Sci 6:4102–4109
25. Corcione CE, Frigione M (2012) UV-cured polymer-boehmite nanocomposite as protective coating for wood elements. Prog Org Coat 74:781–787
26. Greco A, Maffezzoli A, Buccoliero G, Caretto F, Cornacchia G (2012) Thermal and chemical treatments of recycled carbon fibers for improved adhesion to polymeric matrix. J Compos Mater 47:369–377
27. Corcione CE, Freuli F, Maffezzoli A (2013) The aspect ratio of epoxy matrix nanocomposites reinforced with graphene stacks. Polym Eng Sci 53:531–539
28. Daraei P, Madaeni SS, Salehi E, Ghaemi N, Ghari HS, Khadivi MA, Rostami E (2013) Novel thin film composite membrane fabricated by mixed matrix nanoclay/chitosan on PVDF microfiltration support: preparation, characterization and performance in dye removal. J Membr Sci 436:97–108
29. Alexandre M, Dubois P (2000) Polymer-layered silicate nanocomposites: preparation, properties and uses of a new class of materials. Mater Sci Eng 28:1–63
30. Ray SS, Okamoto M (2003) Polymer/layered silicate nanocomposites: a review from preparation to processing. Prog Polym Sci 28:1539–1641
31. De B, Karak N (2013) Novel high performance tough hyperbranched epoxy by an $A_2 + B_3$ polycondensation reaction. J Mater Chem A 1:348–353
32. Kumar M, Gholamvand Z, Morrissey A, Nolan K, Ulbricht M, Lawler J (2016) Preparation and characterization of low fouling novel hybrid ultrafiltration membranes based on the blends of GO−TiO_2 nanocomposite and polysulfone for humic acid removal. J Membr Sci 506:38–49
33. Ma Y, ShiF Wang Z, Wu M, Ma J, Gao C (2012) Preparation and characterization of PSf/clay nanocomposite membranes with PEG 400 as a pore forming additive. Desalination 286:131–137
34. Abdullah N, Gohari RJ, Yusof N, Ismail AF, Juhana J, Lau WJ, Matsuura T (2016) Polysulfone/hydrous ferric oxide ultrafiltration mixed matrix membrane: preparation, characterization and its adsorptive removal of lead (II) from aqueous solution. Chem Eng J 289:28–37
35. Dalwani M, Benes NE, Bargeman G, Stamatialis D, Wessling M (2011) Effect of pH on the performance of polyamide/polyacrylonitrile based thin film composite membranes. J Membr Sci 372:228–238
36. MiaoJ Zhang LC, Lin H (2013) A novel kind of thin film composite nanofiltration membrane with sulfated chitosan as the active layer material. Chem Eng Sci 87:152–159
37. Yu S, Liu M, Ma M, Qi M, Lü Z, Gao C (2010) Impacts of membrane properties on reactive dye removal from dye/salt mixtures by asymmetric cellulose acetate and composite polyamide nanofiltration membranes. J Membr Sci 350:83–91
38. Meihong L, Sanchuan Y, Yong Z, Congjie G (2008) Study on the thin-film composite nanofiltration membrane for the removal of sulfate from concentrated salt aqueous: preparation and performance. J Membr Sci 310:289–295
39. Baroña GNB, Lim J, Jung B (2012) High performance thin film composite polyamide reverse osmosis membrane prepared via *m*-phenylenediamine and 2,2′-benzidinedisulfonic acid. Desalination 291:69–77
40. Chiang YC, Hsub YZ, Ruaan RC, Chuang CJ, Tung KL (2009) Nanofiltration membranes synthesized from hyperbranched polyethyleneimine. J Membr Sci 326:19–26
41. Crock CA, Rogensues AR, Shan W, Tarabara VV (2013) Polymer nanocomposites with graphene-based hierarchical fillers as materials for multifunctional water treatment membranes. Water Res 47:3984–3996
42. Ganesh BM, Isloor AM, Ismail AF (2013) Enhanced hydrophilicity and salt rejection study of graphene oxide-polysulfone mixed matrix membrane. Desalination 313:199–207